Progress In Electromagnetics Research M, Vol. 12, 165–180, 2010

NUMERICAL AND EXPERIMENTAL ANALYSIS OF ELECTROMAGNETIC TORQUE FOR MODULAR TOROIDAL COIL APPLICABLE TO TOKAMAK REACTORS

M. R. Alizadeh Pahlavani, A. Shiri, and A. Shoulaie

Department of Electrical Engineering
Iran University of Science and Technology (IUST)
Tehran, Iran

Abstract—A Modular Toroidal Coil (MTC) is composed of several solenoidal coils (SCs), which are connected in a series and distributed in the toroidal and symmetrical form. This paper presents analytical equations of mutual inductance and electromagnetic torque of the MTC applicable to Tokamak reactors. These equations are based on those formulated by Neumann. The numerical analysis of the integrations resulting from these equations is solved using the extended three-point Gaussian algorithm. The results obtained from the numerical simulation agree with the empirical results, the experimental results, and the virtual work theorem, which indicates the reliability of the presented equations. The behavior of the mutual inductance of the coil shows that the maximum stored energy is obtained when the electromagnetic torque is zero, and vise versa.

1. INTRODUCTION

Recent research in the area of plasma reactors (e.g., Tokamak), Superconductor Magnetic Energy Storage (SMES), and nuclear fusion reactors concerns studying different coils. As an example, Tokamak reactors consist of coils with various structures, such as the modular toroidal (MTC), the helical toroidal, the solenoidal, and the poloidal.

The capability of modular implementation of the MTC is one of its main advantages over the helical toroidal coil. Because the MTC has not been studied as extensively as other coils, the mathematical modeling and analysis of this coil are presented in this paper. The optimal design of an MTC may be carried out using different objective functions such as the minimization of the imposed electromagnetic

Corresponding author: M. R. Alizadeh Pahlavani (Mr_Alizadehp@iust.ac.ir).

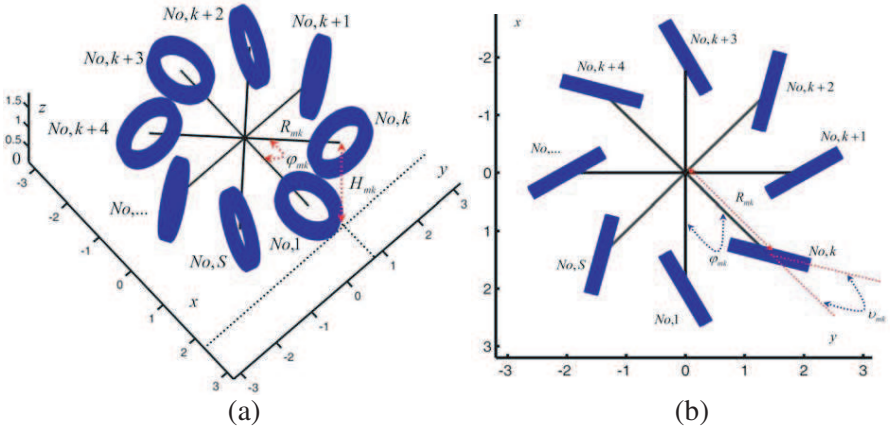

Figure 1. Modular toroidal coil composed of 8 SCs. (a) Three dimensional diagram of the modular toroidal coil. (b) Projection of the structure of the modular toroidal coil on the x-y plane.

torque and translational forces on SCs for an optimized holding fixture design, the maximization of the stored magnetic energy through a determination of mutual inductances, the minimization of the leakage flux, the stabilization of Tokamak reactors, and the elimination of stress. In this article, we present the analytical equations of the mutual inductance and the electromagnetic torque of this coil. Fig. 1 depicts the structure of an MTC with solenoid coils (SCs) that are connected in a series and distributed in the toroidal and the symmetrical form. Fig. 1(b) shows the projection of this coil on the x-y plane.

In this figure, R_{mk} is the distance between the symmetry center of the kth SC from z-axis, υ_{mk} is the angle between R_{mk} direction and the latitudinal axis of the kth SC, φ_{mk} is the toroidal angle of the kth SC, and H_{mk} defines the distance between the longitudinal axis of the kth SC and plane $z = 0$. As mentioned above, usually in the MTC, R_{mi} is assumed constant and $\upsilon_{mi} = 0$ for $i = 1, \ldots, k, \ldots, S$.

The dependency of analytical equations of inductance of the MTC on the geometrical parameters of the SCs such as R_{mi}, $\upsilon_{mi}, \varphi_{mi}, H_{mi}$, $i = 1, \ldots, k, \ldots, S$, when the dimensional parameters of the SCs are known, shows that these parameters can be used as the degrees of freedom of the objective function and thus can be manipulated to satisfy the optimization function.

The structure of this paper is as follows: in Section 2, an appropriate coordinate system for simplifying the mathematical equations is presented, and the longitudinal components of the ring element of each SC in this coordinate system are introduced. In

Section 3, we discuss our study of the analytical equations of the mutual inductance. In Section 4, the numerical results of the mutual inductance are compared with the experimental and empirical results. In Section 5, the analytical equations of electromagnetic torque are presented. Finally, in Section 6, the validity of torque equations is confirmed using virtual work theorem.

2. COORDINATE SYSTEM AND LONGITUDINAL COMPONENTS

Figure 2 shows the ith and the jth hypothetical rings of the MTC with the geometrical parameters of $\upsilon_i, \varphi_i, R_i, a_i, H_i$ and $\upsilon_j, \varphi_j, R_j, a_j, H_j$, respectively. To consider these parameters, the coordinate system should be non-orthogonal, semi-toroidal, three dimensional and rotational, which is named as NSCS by the authors. This new coordinate system is to simplify the mathematical equations. An arbitrary point such as P in the space is defined by ρ, θ, and φ (see Fig. 2). In this coordinate system, unit vectors $\vec{a}_\rho, \vec{a}_\theta$, and $\vec{a}_\varphi$ are defined in the directions ρ, θ,andφ, respectively. Fig. 2 shows the unit vectors of this coordinate system for the point P, located on the ith ring. The Cartesian coordinate system (CCS) of this point can be expressed as Equations (1)–(3) using the projection of the ith ring on the x-y plane as shown in Fig. 3. The longitudinal components of this

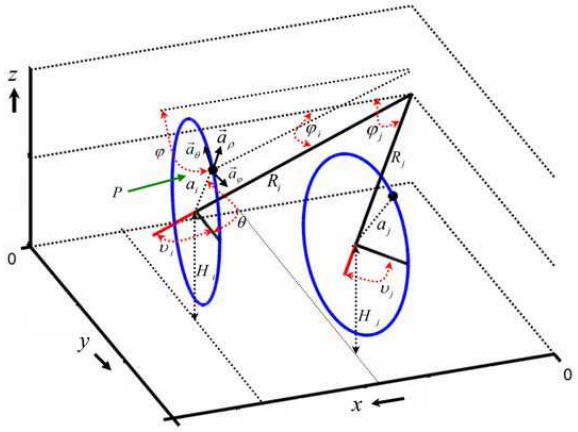

Figure 2. The coordinate system and the two hypothetical rings of the modular toroidal coil.

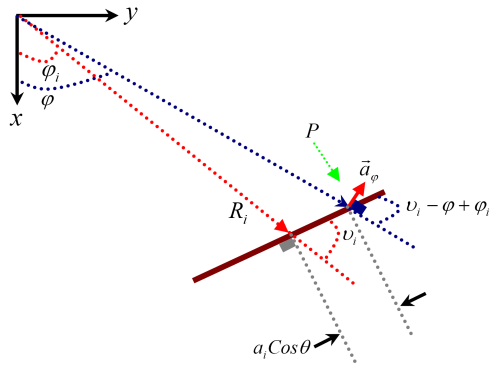

Figure 3. The projection of the th ith ring on the x-y plane.

coordinate system are defined by Equation (4).

$$x_p = (R_i \cos(\varphi - \varphi_i) + a_i \cos\theta \cos(v_i - \varphi + \varphi_i)) \cos\varphi \quad (1)$$

$$y_p = (R_i \cos(\varphi - \varphi_i) + a_i \cos\theta \cos(v_i - \varphi + \varphi_i)) \sin\varphi \quad (2)$$

$$z_p = H_i + a_i \sin\theta \quad (3)$$

$$\begin{aligned} dl_i &= \vec{a}_\varphi(R_i \cos(\varphi-\varphi_i)+a_i \cos\theta\cdot\cos(v_i-\varphi+\varphi_i))d\varphi+\vec{a}_\theta a_i d\theta+\vec{a}\rho d\rho \\ &= \vec{a}_x dl_{ix} + \vec{a}_y dl_{iy} + \vec{a}_z dl_{iz} \end{aligned} \quad (4)$$

where

R_i: the distance between the symmetry center of the ith ring from z-axis;

a_i: the radius of ith ring;

H_i: the distance between the symmetry center of the ith ring from x-y plane;

φ_i: toroidal angle of the symmetry center of ith ring;

v_i: the angle between R_i direction and the latitudinal axes of the ith ring;

ρ, θ, φ: three parameters defining an arbitrary point such as P in the NSCS;

x_p, y_p, z_p: Cartesian coordinates of an arbitrary point such as P in the CCS;

$dl_{ix}, dl_{iy}, dl_{iz}$: longitudinal components of the ith ring;

$\vec{a}_x, \vec{a}_y, \vec{a}_z$: unit vectors of the CCS;

$\vec{a}_\rho, \vec{a}_\theta, \vec{a}_\varphi$: unit vectors of the NSCS.

The dot product of the unit vectors of this coordinate system and the Cartesian coordinate system using the projection of the unit vectors of the two mentioned coordinate systems on the x-y plane are presented in Table 1. The longitudinal components of the ith ring

Table 1. The dot product of the unit vectors for the two mentioned coordinated system.

$\vec{a}_x \bullet \vec{a}_\theta$	$-\sin\theta\cos(v_i-\varphi+\varphi_i)\cos\varphi$
$\vec{a}_x \bullet \vec{a}_\varphi$	$-\sin\varphi$
$\vec{a}_x \bullet \vec{a}_\rho$	$\cos\theta\cos(v_i-\varphi+\varphi_i)\cos\varphi$
$\vec{a}_y \bullet \vec{a}_\theta$	$-\sin\theta\cos(v_i-\varphi+\varphi_i)\sin\varphi$
$\vec{a}_x \bullet \vec{a}_\varphi$	$\cos\varphi$
$\vec{a}_y \bullet \vec{a}_\rho$	$\sin\varphi\cos(v_i-\varphi+\varphi_i)\cos\theta$
$\vec{a}_z \bullet \vec{a}_\theta$	$\cos\theta$
$\vec{a}_z \bullet \vec{a}_\varphi$	0
$\vec{a}_z \bullet \vec{a}_\rho$	$\sin\theta$

element in the Cartesian coordinate system are obtained using Table 1 as Equations (5)–(7). Since the ith ring's geometric loci is given by $\rho = a_i$, the longitudinal components of the ith ring by substitution of $d\rho = 0$ can simplify Equations (4) to (7). Furthermore, the relation between θ and φ for the ith ring and the differential of φ, using Fig. 3 can be expressed as Equations (8) and (9).

$$dl_{ix} = dl_i \cdot \vec{a}_x = -a_i \sin\theta\cos(v_i-\varphi+\varphi_i)\cdot\cos\varphi d\theta + \cos\theta\cos(v_i-\varphi+\varphi_i) \cdot\cos\varphi d\rho - \sin\varphi(R_i\cos(\varphi-\varphi_i) + a_i\cos\theta\cos(v_i-\varphi+\varphi_i))d\varphi \quad (5)$$

$$dl_{iy} = dl_i \cdot \vec{a}_y = -a_i \sin\theta\cos(v_i-\varphi+\varphi_i)\cdot\sin\varphi d\theta + \cos\theta\cos(v_i-\varphi+\varphi_i) \cdot\sin\varphi d\rho + \cos\varphi(R_i\cos(\varphi-\varphi_i) + a_i\cos\theta\cos(v_i-\varphi+\varphi_i))d\varphi \quad (6)$$

$$dl_{iz} = dl_i \cdot \vec{a}_z = a_i\cos\theta d\theta + \sin\theta d\rho \quad (7)$$

$$\varphi = \varphi_i + \tan^{-1}\left(\frac{a_i\cos\theta\sin v_i}{R_i + a_i\cos\theta\cos v_i}\right) \quad (8)$$

$$d\varphi = \frac{-a_i R_i \sin v_i \sin\theta}{R_i^2 + a_i^2\cos^2\theta + 2a_i R_i\cos\theta\cos v_i} d\theta \quad (9)$$

The dependency of the presented equations on the geometrical parameters of the ith ring indicates that the relationship between the geometrical parameters of the kth SC and the geometrical parameters of the rings of the same SC should be defined. In Fig. 4, the latitudinal cross-section of the kth SC of the MTC with the geometrical parameters of this coil, i.e., $v_{mk}, R_{mk}, \varphi_{mk}, H_{mk}$ is shown.

In this figure, the numbers on each ring indicates the sequence of the rings connected in series. As seen in this figure, the kth SC is composed of $N_k M_k$ rings where M_k is the number of the layers and N_k represents the number of the rings in each layer. Knowing

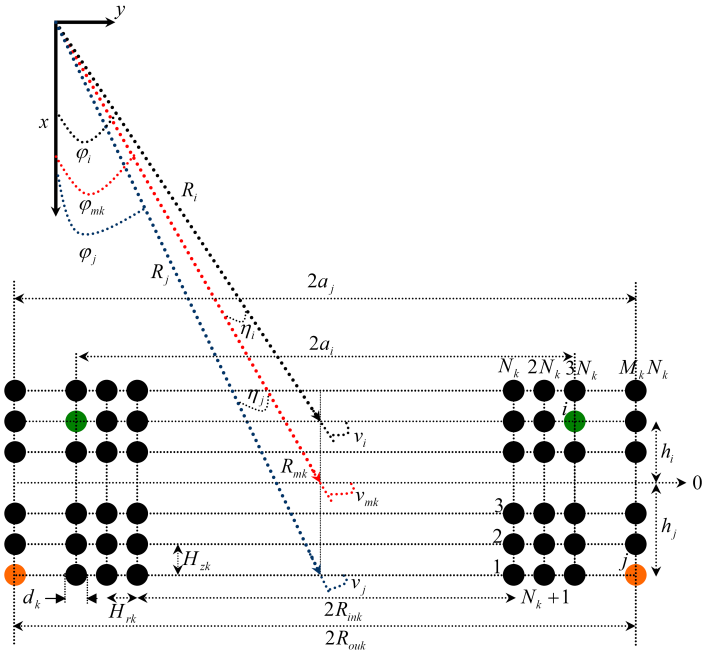

Figure 4. Latitudinal cross-section of the th Kth sc.

the dimensional parameters of the kth SC $(M_k, N_k, d_k, H_{zk}, R_{ouk}, R_{ink})$ and the geometrical parameters of the same coil $(\upsilon_{mk}, R_{mk}, \varphi_{mk}, H_{mk})$, the geometrical parameters of the ith ring, i.e., $\upsilon_i, \varphi_i, R_i, a_i$, and H_i can be derived as Equations (10) to (14). Consequently, the relation between the geometrical parameters of each ring of the MTC with the geometric and the dimensional parameters of the corresponding SCs are given as Equations (10) to (14).

$$\eta_i = \tan^{-1}(h_i \cos \upsilon_{mk}/(R_{mk} - h_i \sin \upsilon_{mk})) \tag{10}$$

$$\varphi_i = \varphi_{mk} + \eta_i \tag{11}$$

$$\upsilon_i = \upsilon_{mk} - \eta_i \tag{12}$$

$$R_i = (R_{mk} - h_i \sin \upsilon_{mk})/\cos \eta_i \tag{13}$$

$$H_i = H_{mk} \tag{14}$$

where

R_{mk}: distance between the symmetry center of the kth SC from z-axis;

φ_{mk}: toroidal angle of the symmetry center of kth SC;

H_{mk}: the distance between the symmetry center of the kth SC from x-y plane;

v_{mk}: the angle between R_{mk} direction and the latitudinal axes of the kth SC;

M_k: the number of the layers of the kth SC;

N_k: the number of rings in each layer of the kth SC;

d_k: the diameter of the conductor of the kth SC;

H_{zk}: the latitudinal distance between two adjacent conductor of the kth SC;

H_{rk}: the longitudinal distance between two adjacent conductor of the kth SC;

R_{ouk}: the radius of the largest ring of the kth SC;

R_{ink}: the radius of the smallest ring of the kth SC;

h_i: the distance between the center of the ith ring from longitudinal symmetrical axes in latitudinal crosssection of the kth SC;

h_j: the distance between the center of the jth ring from longitudinal symmetrical axes in latitudinal crosssection of the kth SC.

3. ANALYTICAL EQUATIONS OF MUTUAL INDUCTANCE

In this section, the analytical equations of mutual inductance between two rings and between two selonoidal coils are presented. Many contributions have been made in the literature to the problem of mutual inductance calculation for coaxial circular coils [1, 2]. Usually, in the classic electrodynamics, the theoretical equations for calculation of mutual inductance are divided into four equations namely, Neumann, Graneaus, Weber, and Maxwell. The mutual inductance of circular rings can be obtained in analytical or semi-analytical forms expressed over elliptical integrals of the first, second, and third kind, Heuman's Lambda function, Bessel functions, and Legendre functions [3]. Considering that the Neumann's equation is brief and to point when compared with other equations, the paper uses this equation to calculate the mutual inductance of two circular rings. Some researchers usually use one of the integrations of the Neumanns' equation, which is presented as linear double integration, to calculate the mutual inductance of two circular rings in a way that by selecting a proper coordinate system, they convert the integration of the Neumann's equation to the first, the second, and the third elliptical integration, if possible. Such researchers solve the second integration of the Neumann's equation as numerically if the integrand is so complicated and the analytical method is not possible or is not easy [4]. Using Neumann's equation (Equation (15)), the mutual

inductance between the ith and the jth ring with the geometrical parameters of $v_i, \varphi_i, R_i, a_i, H_i$ and $v_j, \varphi_j, R_j, a_j, H_j$ can be calculated. Furthermore, the mutual inductance between the kth and the lth SCs are calculated using the current filament [12] via Equation (5).

$$L_{ij} = (\mu_0/4\pi) \oint_{\rho=a_i} \oint_{\rho=a_j} \frac{dl_i \bullet dl_j}{|\chi_{ij}|} = \int_0^{2\pi} \int_0^{2\pi} g(\theta_i, \theta_j) d\theta_i d\theta_j \quad i \neq j \tag{15}$$

$$M_{kl} = \sum_{i=1}^{M_k N_k} \sum_{j=M_k N_k+1}^{M_k N_k + M_l N_l} L_{ij} \tag{16}$$

where in these equations:

$$\chi_{ij} = \chi_x \vec{a}_x + \chi_y \vec{a}_y + \chi_z \vec{a}_z = (x_j - x_i)\vec{a}_x + (y_j - y_i)\vec{a}_y + (z_j - z_i)\vec{a}_z$$

$$g(\theta_i, \theta_j) = \frac{\mu_0 [dl_{ix} dl_{jx} + dl_{iy} dl_{jy} + dl_{iz} dl_{jz}]}{4\pi [(x_i - x_j)^2 + (y_i - y_j)^2 + (z_i - z_j)^2]^{1.5}}$$

$$dl_{ix} dl_{jx} = [-a_i \sin\theta \cos(v_i - \lambda_i + \varphi_i) \cos\lambda_i - \sin\lambda_i (R_i \cos(\lambda_i - \varphi_i) + a_i \cos\theta \cos(v_i - \lambda_i + \varphi_i))\gamma_i] \cdot [-a_j \sin\theta \cos(v_j - \lambda_i + \varphi_j) \cos\lambda_j - \sin\lambda_j (R_i \cos(\lambda_j - \varphi_j) + a_j \cos\theta \cos(v_j - \lambda_j + \varphi_j))\gamma_j]$$

$$dl_{iy} dl_{jy} = [-a_i \sin\theta \cos(v_i - \lambda_i + \varphi_i) \sin\lambda_i + \cos\lambda_i (R_i \cos(\lambda_i - \varphi_i) + a_i \cos\theta \cos(v_i - \lambda_i + \varphi_i))\gamma_i] \cdot [-a_j \sin\theta \cos(v_j - \lambda_i + \varphi_j) \sin\lambda_j + \cos\lambda_j (R_i \cos(\lambda_j - \varphi_j) + a_j \cos\theta \cos(v_j - \lambda_j + \varphi_j))\gamma_j]$$

$$dl_{iz} dl_{jz} = [a_i \cos\theta_i] \cdot [a_j \cos\theta_j]$$

$$\lambda_i = \varphi_i + \tan^{-1}(a_i \cos\theta_i \sin v_i / (R_i + a_i \cos\theta_i \cos v_i))$$

$$\gamma_i = \frac{-a_i R_i \sin v_i \sin\theta_i}{R_i^2 + a_i^2 \cos^2\theta_i + 2a_i R_i \cos\theta_i \cos v_i}$$

$$\lambda_j = \varphi_j + \tan^{-1}(a_j \cos\theta_j \sin v_j / (R_j + a_j \cos\theta_j \cos v_j))$$

$$\gamma_j = \frac{-a_j R_j \sin v_j \sin\theta_j}{R_j^2 + a_j^2 \cos^2\theta_j + 2a_j R_j \cos\theta_j \cos v_j}$$

$$x_i = (R_i \cos(\lambda_i - \varphi_i) + a_i \cos\theta_i \cos(v_i - \lambda_i + \varphi_i)) \cos\lambda_i$$

$$y_i = (R_i \cos(\lambda_i - \varphi_i) + a_i \cos\theta_i \cos(v_i - \lambda_i + \varphi_i)) \sin\lambda_i$$

$$z_i = H_i + a_i \sin\theta_i$$

$$x_j = (R_j \cos(\lambda_i j - \varphi_j) + a_j \cos\theta_j \cos(v_j - \lambda_j + \varphi_j)) \cos\lambda_j$$

$$y_j = (R_j \cos(\lambda_j - \varphi_j) + a_j \cos\theta_j \cos(v_j - \lambda_j + \varphi_j)) \sin\lambda_j$$

$$z_j = H_j + a_j \sin\theta_j$$

M_{kl} the mutual inductance between kth SC and lth SC;
L_{ij} the mutual inductance between ith ring and jth ring;
μ_0 magnetic permeability of vacuum.

4. CONFIRMATION OF NUMERICAL RESULTS USING EXPERIMENTAL RESULTS

MATLAB® m-files are used to simulate the mutual inductance between two rings and two SCs. Numerical integrations of the Equation (15) are performed using the extended three-point Gaussian algorithm [6]. Fig. 5 displays the mutual inductance of two flat

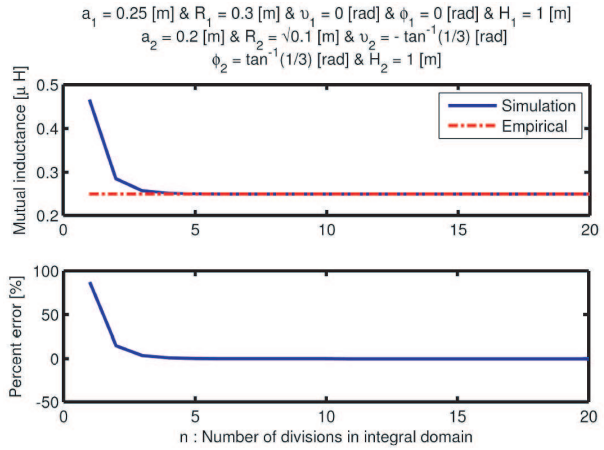

Figure 5. Comparing the empirical and the numerical results of mutual inductance.

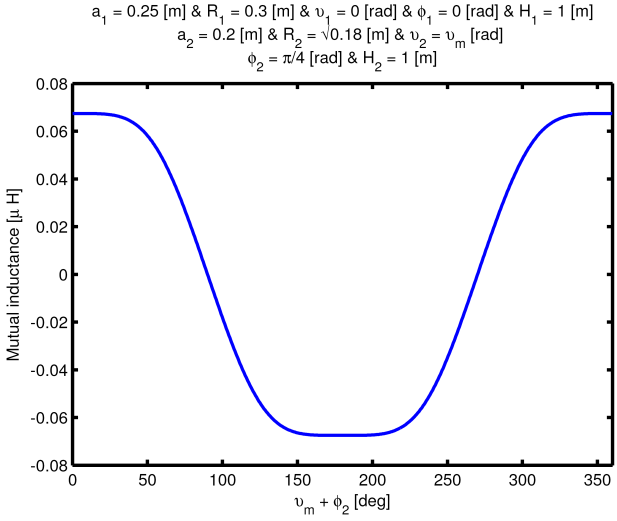

Figure 6. The behavior of the mutual inductance of two coaxial rings.

rings with the radius of 0.2 m and 0.25 m, and with the center-to-center distance of $d = 0.1\,[\mathrm{m}]$ versus n, which n is the number of divisions in the integral domain. It also shows the error resulting from the comparison between the analytical and empirical results [7]. In order to compare the empirical and the numerical results of the same condition, the geometrical parameters of the two rings are obtained as Equation (17). From Fig. 5, it is inferred that the optimum value of n in order to minimize the computation time in the calculation of mutual inductance is 5. Fig. 6 shows the behavior of the mutual inductance between two rings when $\upsilon_2 = \upsilon_m\,[\mathrm{rad}]$ and $\upsilon_1 = 0$. This figure also shows that in a situation in which the surface of the two rings is orthogonal or parallel, the minimum or the maximum mutual inductance is obtained, respectively. Note that these situations occur at $\upsilon_m + \varphi_2 = 90$ or 270 and 0 or 180 [deg]for $d = 0.3\,\mathrm{m}$, respectively.

$$\begin{aligned} &R_1 = 0.3\,[\mathrm{m}], \quad R_2 = \sqrt{d^2 + R_1^2}\,[\mathrm{m}], \\ &\varphi_1 = 0\,[\mathrm{rad}], \quad \varphi_2 = \tan^{-1}(d/R_1)\,[\mathrm{rad}], \\ &\upsilon_1 = 0\,[\mathrm{rad}], \quad \upsilon_2 = -\tan^{-1}(d/R_1)\,[\mathrm{rad}], \end{aligned} \tag{17}$$

where

d: center-to-center distance of two falt rings;

In Fig. 7, the MTC, made from aluminum in the laboratory to validate the presented analytical equations, is depicted.

Figure 8 compares the experimental and the numerical results of the mutual inductance of the two adjacent and similar SCs, connected in series with the dimensional and geometrical parameters shown in Tables 2 and 3 for the two cases $\upsilon_{m1} = 0$, $\upsilon_{m2} = \upsilon_m$ and $\upsilon_{m1} = \upsilon_{m2} = \upsilon_m$.

$\varphi_{mi} = (i-1)\pi/4,\ i = 1, \ldots, 8\,[\mathrm{rad}]$
$R_{mi} = 295,\ i = 1, \ldots, 8\,[\mathrm{mm}]$
$H_{mi} = 1000,\ i = 1, \ldots, 8\,[\mathrm{mm}]$

Table 2. The geometrical parameters of the SCS.

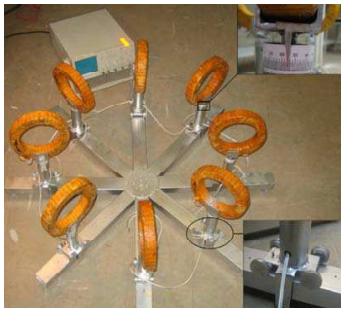

Figure 7. Schematic diagram of the manufactured MTC composed of 8 SCS.

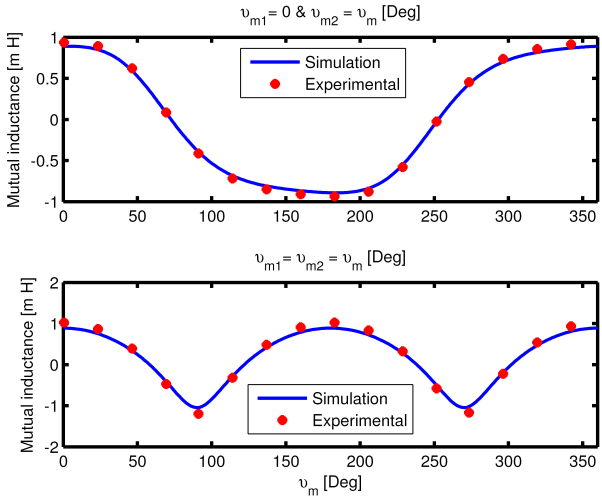

Figure 8. The mutual inductances of two similar and adjacent SCs.

Table 3. Dimensional parameters of the SC.

Dimensional parameters of the solenoid coils	
M_i	16
N_i	20
d_i	1.6 [mm]
H_{zi}	2.1 [mm]
R_{ini}	75 [mm]
R_{oui}	110 [mm]

In this paper, $n = 5$ (optimal integration interval) for the numerical calculation is used. Fig. 8 and Table 4 shows that the experimental results nearly coincide with the analytical equation, which is given in (16) with the average of the error being less than 5%. This error might result from an error in measurement, the value of n, the environmental magnetic field, and so forth.

5. THE ANALYTICAL EQUATIONS OF ELECTROMAGNETIC TORQUE

In this section, the analytical equations of the electromagnetic torque between the ith and the jth ring or between the kth and the lth SCs are presented. It should be noted that if the ith ring or the kth SC are kept constant, then electromagnetic torque will cause the postural movement of the jth ring or the lth SC. It is assumed that the

holding fixture of the SC is able to keep the gravity center of these coils constant. These gravity centers are also considered to be the torque center for the electromagnetic torque analysis purposes. Another assumption is that the ith ring or the kth SC are kept constant, and the jth ring or the lth SC have only one degree of freedom in the direction of υ_j or υ_{ml}. Therefore, the torque of the jth ring in the υ_j direction can be obtained through (18). Also, the torque of the lth SC in the υ_{ml} directions is obtained by adding all the imposed torques on the rings of the lth SC using (19). These equations are based on the Bio-Savart equation by assuming that the torque arm is r_j.

$$
\begin{aligned}
T_{ij} &= T_{ijx}\vec{a}_x + T_{ijy}\vec{a}_y + T_{ijz}\vec{a}_z = \oint_{\rho=aj} dT = \oint_{\rho=aj} r_j \times dF \\
&= \oint_{\rho=aj} r_j \times I_j dl_j \times B_{ij} = \oint_{\rho=aj} r_j \times I_j dl_j \times \oint_{\rho=ai} (\mu_0/4\pi) I_i dl_i \times \left(a_{\chi ij}/|\chi_{ij}|^2\right) \\
&= (\mu_0 I_i I_j/4\pi) \oint_{\rho=aj} \oint_{\rho=ai} r_j \times dl_j \times dl_i \times \left(a_{\chi ij}/|\chi_{ij}|^2\right) \\
&= (\mu_0 I_i I_j/4\pi) \int_0^{2\pi} \int_0^{2\pi} (t_x\vec{a}_x + t_y\vec{a}_y + t_z\vec{a}_z) d\theta_i d\theta_j
\end{aligned} \tag{18}
$$

$$
T = T_x\vec{a}_x + T_y\vec{a}_y + T_z\vec{a}_z = \sum_{i=1}^{M_k N_k} \sum_{j=M_k N_k+1}^{N_k N_k + M_l N_l} T_{ij} \tag{19}
$$

where in these equation;

$$
\begin{aligned}
r_j &= r_x\vec{a}_x + r_y\vec{a}_y + r_z\vec{a}_z \\
&= (x_j - R_j\cos\varphi_j)\vec{a}_x + (y_j - R_j\sin\varphi_j)\vec{a}_y + (z_j - H_j)\vec{a}_z \\
t_x &= -r_y\chi_z(dl_{iy}dl_{jy} + dl_{ix}dl_{jx}) + r_z\chi_y(dl_{ix}dl_{jx} + dl_{iz}dl_{jz}) \\
&+ r_y dl_{iz}(\chi_x dl_{jx} + \chi_y dl_{jy}) - r_z dl_{iy}(\chi_x dl_{jx} + \chi_z dl_{jz}) \\
t_y &= -r_z\chi_x(dl_{iz}dl_{jz} + dl_{iy}dl_{jy}) + r_x\chi_z(dl_{iy}dl_{jy} + dl_{ix}dl_{jx}) \\
&+ r_z dl_{ix}(\chi_z dl_{jz} + \chi_y dl_{jy}) - r_x dl_{iz}(\chi_x dl_{jx} + \chi_y dl_{jy}) \\
t_z &= -r_x\chi_y(dl_{iz}dl_{jz} + dl_{ix}dl_{jx}) + r_y\chi_x(dl_{iy}dl_{jy} + dl_{iz}dl_{jz}) \\
&+ r_x dl_{iy}(\chi_z dl_{jz} + \chi_x dl_{jx}) - r_y dl_{ix}(\chi_z dl_{jz} + \chi_y dl_{jy})
\end{aligned}
$$

I_i: the current of the ith ring;
I_j: the current of the jth ring.

Table 4. Confirmation of numerical results using experimental results.

Mutual inductance $\upsilon_1 = 0, \quad \upsilon_2 = \upsilon_m$ [deg]			**Electromagnetic torque in z direction** $\upsilon_1 = 0, \quad \upsilon_2 = \upsilon_m$ [deg]		
υ_m [deg]	Num. [mH]	Exp. [mH]	υ_m [deg]	Num. [$m\ Nm$]	Exp. [$m\ Nm$]
0	0.8914	0.9395	0	0.0376	0.0396
			11	0.0646	0.0678
23	0.8497	0.8939	23	0.2708	0.2830
			34	0.6077	0.6350
46	0.5930	0.6221	46	1.0149	1.0646
			57	1.3360	1.4055
69	0.0804	0.0840	69	1.4238	1.5007
			80	1.2766	1.3455
91	0.3943	0.4120	92	0.9930	1.0466
			103	0.6923	0.7297
114	0.6833	0.7168	115	0.4489	0.4722
			126	0.2835	0.2974
137	0.8089	0.8510	137	0.1850	0.1933
			149	0.1320	0.1379
160	0.8662	0.9130	160	0.1024	0.1074
			172	0.0733	0.0771
$\upsilon_1 = \upsilon_2 = \upsilon_m$ [deg]			$\upsilon_1 = \upsilon_2 = \upsilon_m$ [deg]		
0	0.8911	0.9392	0	0.0376	0.0396
			11	0.1603	0.1682
23	0.7530	0.7922	23	0.4256	0.4448
			34	0.7348	0.7679
46	0.3401	0.3568	46	1.0620	1.1140
			57	1.3692	1.4404
69	0.4105	0.4290	69	1.5342	1.6170
			80	1.0934	1.1524
91	1.0408	1.0876	92	0.4419	0.4658
			103	1.0077	1.0621
114	0.2785	0.2921	115	0.6917	0.7277
			126	0.4241	0.4449
137	0.4194	0.4412	137	0.2932	0.3064
			149	0.2405	0.2513
160	0.7897	0.8323	160	0.2032	0.2132
			172	0.1300	0.1368

6. VALIDITY OF THE ANALYTICAL EQUATIONS OF ELECTROMAGNETIC TORQUE USING VIRTUAL WORK THEOREM

Figure 9 and Table 4 depicts the imposed electromagnetic torque components on the second SC for $\upsilon_{m1} = 0$, $\upsilon_{m2} = \upsilon_m$, and $\upsilon_{m1} = \upsilon_{m2} = \upsilon_m$, versus υ_m using Equation (19) and $n = 5$.

As shown in this figure, the torque component in the x and the y directions (T_x and T_y) are zero. This is because they do not posses any degree of freedom in these directions. Also, the electromagnetic

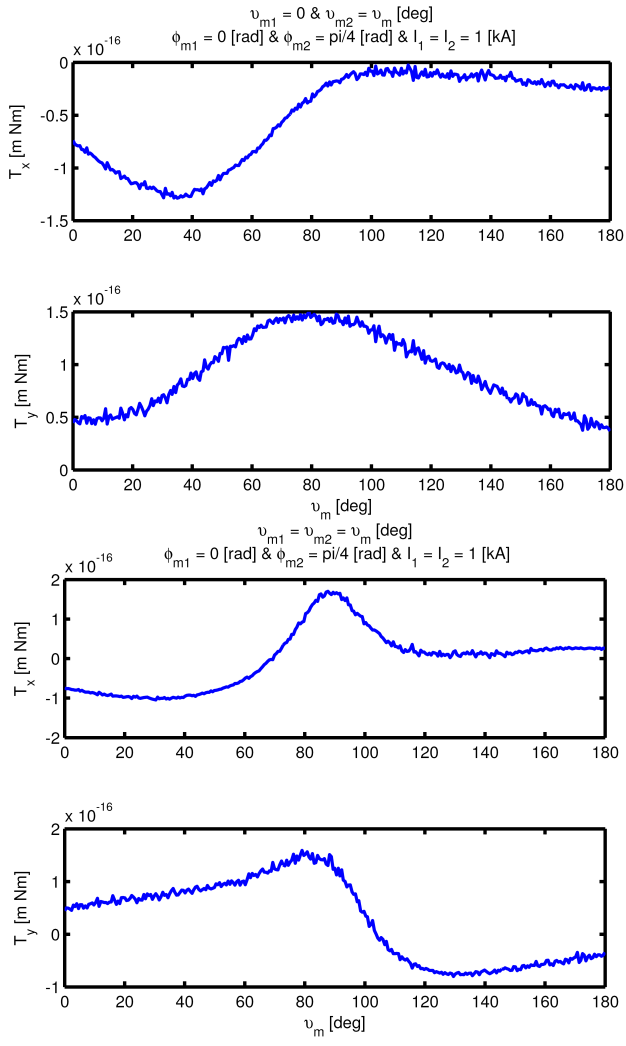

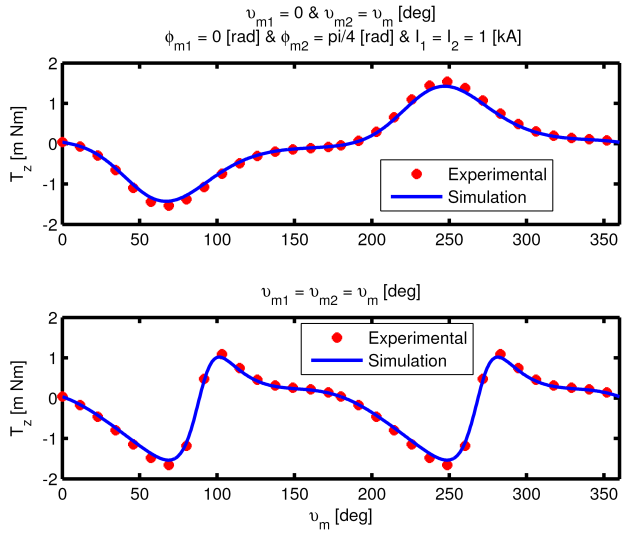

Figure 9. The behavior of the imposed electromagnetic torque on the second solenoidal coil for cases $\upsilon_{m1} = 0, \upsilon_{m2} = \upsilon_m$ [deg] and $\upsilon_{m1} = \upsilon_{m2} = \upsilon_m$ [deg].

torque using the virtual work theorem in a magnetic structure, in which the stored magnetic energy varies with its freedom degrees, is defined as (20). Since in two SCs connected in series, only mutual inductance varies with υ_m, Equation (20) can be expressed as (21). It is noted that the self-inductance of the coils remains constant when υ_m varies, so its differential with respect to υ_m is zero.

$$T_z = \frac{\partial W_m}{\partial \upsilon_m} \tag{20}$$

$$T_z = I_k I_l \frac{\partial M_{kl}}{\partial \upsilon_m} = I_1 I_2 \frac{\partial M_{12}}{\partial \upsilon_m} \tag{21}$$

Therefore, the differential of the experimental results of the mutual inductance between two adjacent SCs connected in series will result in the torque in z direction, and these results can be compared with the torque that resulted from Equation (19), shown in Fig. 9. A comparison of Fig. 8 and Fig. 9 shows that the maximum stored magnetic energy occurs when the electromagnetic torque is zero and the mutual inductance is maximum while the minimum energy is obtained when the electromagnetic torque is maximum (the mutual inductance is zero). Moreover, Fig. 9 indicates that the presented analytical equations to determine the electromagnetic torque are highly reliable, and it fully agrees with the virtual work theorem with an error of less than 8%.

7. CONCLUSION

This paper presents analytical equations of mutual inductance and electromagnetic torque of the MTC applicable to Tokamak reactors. The MATLAB program was used for a numerical simulation of mutual inductance and electromagnetic torque. The numerical results and the experimental results of mutual inductance and also the numerical results, which are obtained based on the virtual work theorem, are compared in order to validate the presented equations. This comparison shows that the obtained errors for mutual inductance and electromagnetic torque are less than 5%, and 8%, respectively. Therefore, the proposed equations are highly reliable.

REFERENCES

1. Babic, S. I. and C. Akyel, "New mutual inductance calculation of the magnetically coupled coils: Thin disk coil-thin wall solenoid," *Journal of Electromagnetic Waves and Applications*, Vol. 20, No. 10, 1661–1669, 2006.
2. Akyel, C., S. I. Babic, and M.-M. Mahmoudi, "Mutual inductance calculation for noncoaxial circular air coils with parallel axes," *Progress In Electromagnetics Research*, PIER 91, 287–301, 2009.
3. Zhao, P. and H. G. Wang, "Resistances and inductances extraction using surface integral equation with the acceleration of multilevel green function interpolation method," *Progress In Electromagnetics Research*, PIER 83, 43–54, 2008.
4. Babic, S. I. and C. Akyel, "Calculating mutual inductance between ircular coils with inclined axes in air," *IEEE Trans. on Magnetics*, Vol. 4, No. 7, 1743–1750, Jul. 2008.
5. Babic, S., C. Akyel, and S. J. Salon, "New procedures for calculating the mutual inductance of the system: Filamentary circular coil-massive circular solenoid," *IEEE Trans. Magn.*, Vol. 39, No. 3, 1131–1134, May 2003.
6. Pennington, R. H., *Introductory Computer Methods and Numerical Analysis*, 4th Edition, Macmillan, New York, 1970.
7. Grover, F. W., *Inductance Calculation Working Formulas and Tables*, 77–87, Dover Publications, Inc., New York, 1946.